

(tn)₂][M(CN)₄]³⁻ (en = ethylenediamine; tn = 1,3-diaminopropane; M = Ni, Pd, Pt). In both cases the three salts are isostructural (X-ray powder diffraction), and there is no Pt-Pt interaction in the mixed salts. Consequently, the differences may be attributed to Pt-Pt interactions in the mixed complex salts that produce distortion in the lattice due to the packing, there is more free space, and the escape of a water molecule will be easier.

The E_a values for the Ni and Pd compounds agree with the described value⁵ for [Co(H₂O)(NH₃)₅][Co(CN)₆], 143.8 ± 7 kJ/mol, where interstitial diffusion of water molecules as Frenkel defects is not enhanced by the similarity of the two ions. The values reported by LeMay² for chloride, bromide, and nitrate compounds (about 85–90 kJ/mol) are intermediate between our values found for the Ni and Pd compounds and that for the Pt compound. We can conclude that the proposed S_N1 mechanism is more accurate in complexes of the aquopentaamminecobalt(III) cation; the activated complex is a square-based pyramid, and the action energy can vary depending on the crystal structures and relative sizes of the anion and cation.

Furthermore, the entropy of activation calculated from the expression

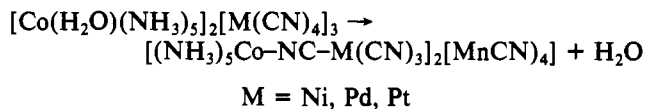
$$(\ln K)h/(k_B T) = \Delta S^\ddagger / R - \Delta H^\ddagger / RT \quad (K = \text{rate constant})$$

also may indicate the differences between the Ni and Pd compounds and the Pt compound (Table III). According to House⁹ the entropy effect may also be explained by the relative sizes (in our case the relative packing) of the ions and the free volume: where there is a large space between the cations and anions (as we suppose in the Pt compound), the water molecule may be able to slip into a interstitial position, causing little or no lattice distortion. Therefore the entropy of activation may be small or slightly negative. Where there is a smaller space between the ions (as we can suppose in the Ni and Pd

compounds), the water molecules can occupy an interstitial position only with considerable lattice expansion so that the entropy of activation is positive. Although this entropy reasoning of House is speculative and not supported by any facts, we believe that it gives an intuitive comprehension of the process.

Conclusions

A dissociative mechanism for the deaquation-anation reaction



is proposed from TG measurements (isothermal and nonisothermal), but the calculated activation energy is of the same magnitude only for the Ni and Pd compounds, being very different in the Pt compound. To explain this difference, and taking into account the similarity of the anions, we propose a different structure in the Pt case that allows the water molecule to escape easily from the crystal lattice. This difference may be due to Pt-Pt interactions in the solid state as shown by the appearance of the new, very intense band at 355 nm in the electronic spectrum (a similar band also appears in dilute solution). The Pt-Pt interactions can produce distortions in the lattice (similar to Peierls distortions) which would be responsible for the different behavior on heating.

Registry No. [Co(H₂O)(NH₃)₅]₂[Ni(CN)₄]₃, 90269-67-3; [Co(H₂O)(NH₃)₅]₂[Pd(CN)₄]₃, 90269-68-4; [Co(H₂O)(NH₃)₅]₂[Pt(CN)₄]₃, 90269-69-5; [(NH₃)₅Co-NC-Ni(CN)₃]₂[Ni(CN)₄], 90269-71-9; [(NH₃)₅Co-NC-Pd(CN)₃]₂[Pd(CN)₄], 90269-73-1; [(NH₃)₅Co-NC-Pt(CN)₃]₂[Pt(CN)₄], 90269-75-3; [Co(H₂O)(NH₃)₅](ClO₄)₃, 13820-81-0; K₂[Ni(CN)₄], 14220-17-8; K₂[Pd(CN)₄], 14516-46-2; K₂[Pt(CN)₄], 562-76-5.

Supplementary Material Available: A listing of kinetic parameters calculated for each compound (both nonisothermal and isothermal methods) for all the principal expressions for growth, nucleation, nucleation-growth, and diffusion mechanisms (71 pages). Ordering information is given on any current masthead page.

(32) Ribas, J.; Serra, M., to be submitted for publication. The activation energy for the three compounds is about 120–130 kJ/mol.

Contribution from the Department of Inorganic Chemistry,
Indian Association for the Cultivation of Science, Calcutta 700032, India

Hydroxamates of Bis(2,2'-bipyridine)ruthenium: Synthesis, Protic, Redox, and Electroprotic Equilibria, Spectra, and Spectroelectrochemical Correlations

PHALGUNI GHOSH and ANIMESH CHAKRAVORTY*

Received July 20, 1983

The synthesis and characterization of pink complexes of the type Ru^{II}(bpy)₂(RX)ClO₄·2H₂O are reported (bpy = 2,2'-bipyridine; RX = RN(O)C(O)C₆H₄-*p*-X; R = H, Me; X = OMe, Me, H, Cl, NO₂). The HX complexes act as weak acids in aqueous media; the pK values (8–11) correlate linearly with σ , the Hammett substituent constant of X. The green deprotonated complex Ru^{II}(bpy)₂(X)·H₂O has been isolated. All species show highly reversible ruthenium(III)–ruthenium(II) couples in acetonitrile with formal potentials, E°_{298} , that vary (–0.3 to 0.5 V) linearly with σ but with a relatively small reaction constant (~0.08 V). The E°_{298} values of the deprotonated complexes are unusually low; the complexes also display a reversible ruthenium(IV)–ruthenium(III) couple ($E^\circ_{298} \sim 0.9$ V). The ruthenium(IV) complex is, however, relatively unstable. In aqueous media spontaneous proton dissociation occurs on metal oxidation. The resultant electroprotic equilibrium Ru(bpy)₂(X)⁺ + e⁻ + H⁺ ⇌ Ru(bpy)₂(HX)⁺ has been characterized ($E^\circ_{298} \sim 0.5$ V) by using variable-pH cyclic voltammetry in 60:40 water-dioxane. The complexes Ru^{III}(bpy)₂(MeMe)(ClO₄)₂·2H₂O (blue) and Ru^{III}(bpy)₂(H)ClO₄·2H₂O (brownish yellow) are isolated by oxidation of the ruthenium(II) counterparts with cerium(IV) in neutral aqueous acetonitrile. All ruthenium(II) complexes have an MLCT band system in the visible region (530–720 nm). Deprotonation markedly affects the MLCT band energy as it does metal redox potentials. The linear correlation of the MLCT frequency with the difference of E°_{298} of metal oxidation (Ru(II) → Ru(III)) and bpy reduction (bpy → bpy⁻) is noted.

Introduction

The structure and stereochemistry and formation and stability as well as transport and reactivity of the hydroxamates of transition-metal ions have been the subject of many recent

studies.^{1–4} This interest originates from several factors such as the analytical usefulness of hydroxamates⁵ and particularly

(1) Smith, W. L.; Raymond, K. N. *J. Am. Chem. Soc.* **1981**, *103*, 3341.

Table I. Complexes and Their Characterization

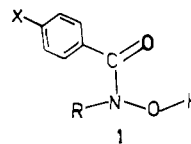
R	X	$\Lambda_M^a / \Omega^{-1} \text{ cm}^2 \text{ M}^{-1}$	$\nu_{\text{C=O}}^b / \text{cm}^{-1}$	analysis ^c		
				% C	% H	% N
Ru(bpy) ₂ (RX)ClO ₄ ·2H ₂ O						
Me	OMe	170	1580	47.66 (47.76)	4.20 (4.22)	9.55 (9.60)
Me	Me	190	1560	48.78 (48.84)	4.21 (4.26)	9.80 (9.82)
Me	H	160	1570	49.14 (48.09)	4.17 (4.00)	9.97 (10.02)
Me	Cl	200	1570	49.83 (49.92)	3.81 (3.68)	9.66 (9.56)
Me	NO ₂	180	1570	45.08 (45.18)	3.75 (3.63)	11.09 (11.29)
H	OMe	170	1560	47.16 (47.01)	3.81 (3.92)	9.64 (9.79)
H	Me	180	1580	48.81 (48.84)	4.18 (4.21)	9.91 (9.82)
H	H	150	1560	47.32 (47.33)	3.81 (3.79)	10.31 (10.22)
H	Cl	160	1580	45.12 (45.05)	3.56 (3.47)	9.88 (9.73)
H	NO ₂	180	1570	44.26 (44.14)	3.36 (3.42)	11.62 (11.51)
Ru(bpy) ₂ (X)·H ₂ O						
	OMe	<i>d</i>	1520	56.55 (56.36)	4.30 (4.19)	11.87 (11.74)
	H	<i>d</i>	1500	57.28 (57.23)	3.99 (4.09)	12.44 (12.36)
	NO ₂	<i>d</i>	1530	53.12 (53.02)	3.85 (3.76)	13.66 (13.74)
Ru(bpy) ₂ (RX)(ClO ₄) ₂ ·2H ₂ O						
Me	Me	280	1590	42.71 (42.85)	3.59 (3.69)	8.68 (8.62)
Ru(bpy) ₂ (X)ClO ₄ ·2H ₂ O						
	H	170	1530	55.17 (55.62)	4.41 (4.29)	12.17 (12.02)

^a Solvent is MeCN. ^b In KBr disk (4000–400 cm⁻¹). ^c Calculated values are in parentheses. ^d Nonelectrolyte.

the siderophoric activity of macrochelate hydroxamic acids in bacterial iron transport.^{6,7} The iron chelates have thus received special attention.^{3,8} Numerous hydroxamates of virtually all elements of the 3d series⁴ as well as those of certain lanthanide⁹ and actinide elements^{1,10} have been examined at varying levels of thoroughness. In contrast, substantial reports on the hydroxamates of 4d and 5d elements are sparse.^{11–14} We have therefore undertaken a project in this area. Aspects of the chemistry of molybdenum hydroxamates^{14–16} were recently reported¹⁷ from this laboratory. In the present work we explore the binding of ruthenium(II), -(III), and -(IV) to hydroxamates¹⁸ using 2,2'-bipyridine (bpy) as a coligand. The synthesis, spectra, protic and redox equilibria, and the coupling of the two into electroprotic equilibria are reported for selected groups of complexes. The effect of remote substituents on such equilibria and the correlation of MLCT (Ru → bpy) transition energies with formal potentials of metal oxidation and bpy reduction are examined.

Results and Discussion

A. The Parent Complexes. The hydroxamic acids concerning us in the present study are of type 1 in which R is H

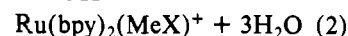


or Me and X is OMe, Me, H, Cl, or NO₂. The acids are abbreviated as HRX where H is the OH proton that invariably dissociates on complex formation. When R = H, the NH proton is potentially dissociable on complexation—a topic considered later in this work.

Ligands of the type HHX react smoothly with Ru(bpy)₂CO₃ in aqueous ethanol, yielding a pink solution of Ru(bpy)₂(HX)⁺ (eq 1), which has been isolated as its perchlorate dihydrate. In contrast HMeX is too weak to react directly with the carbonate complexes; dilute H₂SO₄ is first added to Ru(bpy)₂CO₃, and the diaquo complex thus generated in situ is then reacted with HMeX in the presence of NaOH (eq 2). The pink hydroxamate Ru(bpy)₂(MeX)⁺ is



again isolated as the dihydrated perchlorate salt. Attempted application of reaction 2 rather than 1 to the synthesis of Ru(bpy)₂(HX)⁺ gives a product that is contaminated with deprotonated species (see below). In both synthetic methods the temperature must not rise above 298 K since nitrosyl complexes (identified by IR spectra but not fully characterized) are then formed as contaminants.



again isolated as the dihydrated perchlorate salt. Attempted application of reaction 2 rather than 1 to the synthesis of Ru(bpy)₂(HX)⁺ gives a product that is contaminated with deprotonated species (see below). In both synthetic methods the temperature must not rise above 298 K since nitrosyl complexes (identified by IR spectra but not fully characterized) are then formed as contaminants.

All 10 complexes synthesized (Table I) are diamagnetic and are more soluble in polar organic solvents than in water. In solution they behave as 1:1 electrolytes. Representative conductivity data in acetonitrile are in Table I. In the infrared region we note the decrease in ν_{CO} on going from the free

- Abu-Dari, K.; Raymond, K. N. *Inorg. Chem.* **1980**, *19*, 2034.
- Ghosh, P.; Chakravorty, A. *Inorg. Chim. Acta* **1981**, *56*, L77 and unpublished results.
- Chatterjee, B. *Coord. Chem. Rev.* **1978**, *26*, 281.
- Majumder, A. K. *Int. Ser. Monogr. Anal. Chem.* **1971**, *50*.
- Neilands, J. B., Ed. "Microbial Iron Metabolism"; Academic Press: New York, 1974.
- Raymond, K. N. *Adv. Chem. Ser.* **1977**, *No. 162*.
- Abu-Dari, K.; Cooper, C. J.; Raymond, K. N. *Inorg. Chem.* **1978**, *17*, 3394. Carrano, C. J.; Raymond, K. N.; Harris, W. R. *J. Am. Chem. Soc.* **1979**, *101*, 2722. Raymond, K. N.; Carrano, C. J. *Acc. Chem. Res.* **1979**, *12*, 183. Cooper, S. R.; McArdle, J. V.; Raymond, K. N. *Proc. Natl. Acad. Sci. U.S.A.* **1978**, *75*, 3551.
- Agrawal, Y. K.; Shukla, J. P. *J. Indian Chem. Soc.* **1974**, *51*, 373. Bhatt, K.; Agrawal, Y. K. *Synth. Inorg. Met.-Org. Chem.* **1972**, *2*, 175. Agrawal, Y. K.; Kapoor, H. P. *J. Indian Chem. Soc.* **1976**, *53*, 174.
- Smith, W. L.; Raymond, K. N. *J. Inorg. Nucl. Chem.* **1979**, *41*, 1437. Ghosh, N. N.; Sarkar, D. K. *J. Indian Chem. Soc.* **1968**, *45*, 550. *Ibid.* **1969**, *46*, 528.
- Jones, L. W.; Hard, C. D. *J. Am. Chem. Soc.* **1921**, *43*, 2422.
- Bag, S. P.; Lahiri, S. *J. Inorg. Nucl. Chem.* **1976**, *38*, 1611.
- Mishra, R. S. *J. Indian Chem. Soc.* **1967**, *44*, 400. *Ibid.* **1969**, *46*, 1074.
- Dutta, R. L.; Chatterjee, B. *J. Indian Chem. Soc.* **1967**, *44*, 780.
- Weighardt, K.; Holzbach, W.; Hafer, E.; Weiss, J. *Inorg. Chem.* **1981**, *20*, 343.
- Brewer, G. A.; Sinn, E. *Inorg. Chem.* **1981**, *20*, 1823.
- Ghosh, P.; Chakravorty, A. *Inorg. Chem.* **1983**, *22*, 1322.
- There has been a claim¹³ about the synthesis of Ru(HH)₃. We are unable to reproduce the reported results. The synthesis and study of tris(hydroxamato)ruthenium(III) are in progress in this laboratory.

- Weaver, T. R.; Meyer, T. J.; Adeyemi, S. A.; Brown, G. M.; Ecborg, R. P.; Hatfield, W. E.; Johnson, E. C.; Murray, R. W.; Untereker, D. *J. Am. Chem. Soc.* **1975**, *97*, 3039.

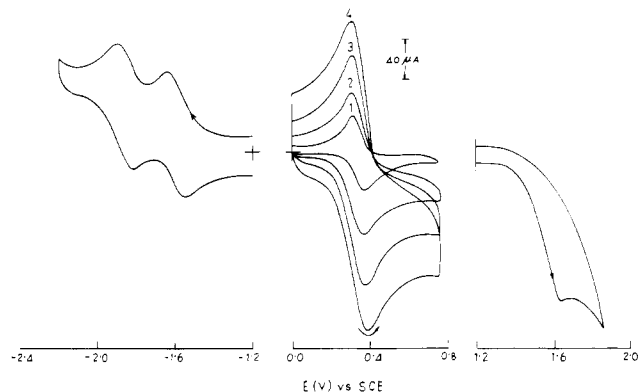
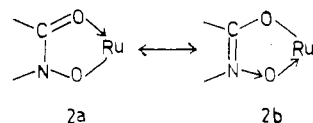


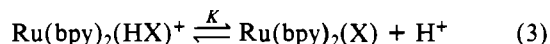
Figure 1. Cyclic voltammograms of $\text{Ru}(\text{bpy})_2(\text{MeMe})\text{ClO}_4 \cdot 2\text{H}_2\text{O}$ in acetonitrile (0.1 M TEAP) at platinum (0.0–2.2 V) and glassy-carbon (0.0 to –2.6 V) electrodes. The responses due to the ruthenium(III)–ruthenium(II) couple are shown at several scan rates (mV s^{-1}): (1) 50; (2) 200; (3) 500; (4) 1000. The other responses are recorded at 50 mV s^{-1} (positive side) and at 100 mV s^{-1} (negative side).

ligand ($1600\text{--}1650 \text{ cm}^{-1}$) to the complexes ($1560\text{--}1590 \text{ cm}^{-1}$; Table I). At least a part of this decrease is believed to be due to the resonance $2\text{a} \leftrightarrow 2\text{b}$. The effect is however less dramatic



than that in the case of $\text{MoO}_2(\text{RX})_2$.¹⁷ The present results taken in conjunction with other infrared data^{1,20} and X-ray data for a number of systems^{1,2,15,16} demonstrate that this type of resonance occurs more or less generally among metal hydroxamates.

B. Protic Equilibria in $\text{Ru}(\text{bpy})_2(\text{HX})^+$. The acid dissociation equilibrium (3) has been studied in 60:40 water–dioxane mixtures (1 M in NaCl). The pK values in the three

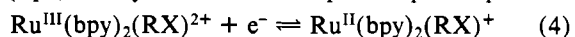


cases examined are as follows: $\text{X} = \text{OMe}$, 10.35 ± 0.05 ; $\text{X} = \text{H}$, 9.90 ± 0.05 ; $\text{X} = \text{NO}_2$, 8.60 ± 0.05 . The data correlate linearly with the Hammett substituent constants of X .

The lability of the NH proton due to complexation of the primary hydroxamate function is qualitatively recognized among e.g. iron⁸ and chromium²¹ hydroxamates. Quantitative results were recently reported¹⁷ by us for one complex of molybdenum: $\text{MoO}_2(\text{HH})_2$, $\text{pK}_1 = 3.45 \pm 0.05$ and $\text{pK}_2 = 5.89 \pm 0.05$. The ruthenium complex $\text{Ru}(\text{bpy})_2(\text{HH})^+$ is a much weaker acid in spite of the net positive charge on the complex and the potential presence of Ru–bpy back-bonding.²² The disparity in the metal oxidation states (Mo(VI), Ru(II)) is clearly the controlling factor here.

The nonelectrolytic deprotonated complexes $\text{Ru}(\text{bpy})_2(\text{X})$ are bottle green in color and can be isolated in the pure form. Physical data for the complexes are in Table I. Here, the CO stretching frequency is even lower than that of $\text{Ru}(\text{bpy})_2(\text{HX})^+$. The deprotonated analogue of 2b probably contributes more¹ to the resonance in $\text{Ru}(\text{bpy})_2\text{X}$.

C. Redox Equilibria. (a) Low Metal Oxidation Potentials. In cyclic voltammetry (CV) the ruthenium(III)–ruthenium(II) couple (eq 4) is fully reversible with a peak-to-peak separation



of 60 mV at scan rates of at least up to 1 V s^{-1} (Figure 1; Table

Table II. Electrochemical Results^{a,b} in Acetonitrile at 298 K

R	X	metal oxidn			bpy redn ^f $-E_{298}^\circ/\text{V}$ ($\Delta E_p/\text{mV}$)
		$E_{298}^\circ(\text{Ru(III)}/\text{Ru(II)})^c/\text{V}$	$n_1^{d,e}$	$n_2^{d,e}$	
$\text{Ru}(\text{bpy})_2(\text{RX})\text{ClO}_4 \cdot 2\text{H}_2\text{O}$					
Me	OMe	0.33	0.98	0.96	1.59 (90), 1.85 (100)
Me	Me	0.34	0.97	0.95	1.59 (80), 1.84 (70)
Me	H	0.35	0.99	0.94	1.59 (80), 1.84 (60)
Me	Cl	0.37	1.01	0.96	1.59 (70), 1.84 (80)
Me	NO_2^h	0.42	0.99	0.98	1.59 (70), 1.84 (90)
H	OMe	0.35	1.02	0.97 ^g	1.63 (70), 1.94 (80)
H	Me	0.35	0.98	0.95 ^g	1.61 (60), 1.91 (60)
H	H	0.37	0.96	0.95 ^g	1.62 (80), 2.1 (80)
H	Cl	0.39	1.05	1.00 ^g	1.62 (80), 2.1 (70)
H	NO_2^h	0.45	0.98	0.96 ^g	1.63 (60), 1.94 (80)
$\text{Ru}(\text{bpy})_2(\text{RX})(\text{ClO}_4)_2 \cdot 2\text{H}_2\text{O}$					
Me	Me	0.34		0.97	1.59 (70), 1.85 (90)

^a Meaning of symbols are as in text. ^b Supporting electrolyte TEAP (0.1 M); solute concentration $\sim 10^{-3} \text{ M}$. Unless otherwise stated, all measurements are made at a platinum working electrode. ^c From cyclic voltammetry: scan rates 50 mV s^{-1} – 1 V s^{-1} ; $\Delta E_p = 60 \text{ mV}$ over the entire range of scan rates. ^d $n_1 = Q/Q'$, where Q' is the calculated coulomb count for 1e transfer and Q is the coulomb count found after exhaustive coulometric oxidation using a platinum-wire gauge at 0.7 V; n_2 is the corresponding number after rereduction of the oxidized solution at 0.0 V. ^e In each case solute concentration is 0.01 mmol, supporting electrolyte is TEAP (0.1 M), and coulometric data are averages of three independent measurements. ^f Glassy-carbon electrode: scan rate 100 mV s^{-1} . ^g At -0.5 V due to deprotonation of the oxidized complex. ^h Quasi-reversible 1e nitro reductions are observed at $R = \text{Me}$, -1.22 V , $\Delta E_p = 70 \text{ mV}$ and $R = \text{H}$, -0.98 V , $\Delta E_p = 70 \text{ mV}$.

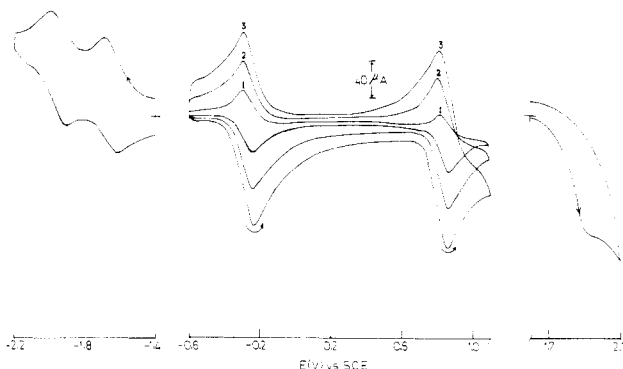


Figure 2. Cyclic voltammograms of $\text{Ru}(\text{bpy})_2(\text{H}) \cdot \text{H}_2\text{O}$ in acetonitrile (0.1 M TEAP) at platinum (0.0–2.2 V) and glassy-carbon (0.0 to –2.6 V) electrodes. The ruthenium(IV)–ruthenium(III) and ruthenium(III)–ruthenium(II) couples are shown at several scan rates (mV s^{-1}): (1) 50; (2) 200; (3) 500. The other responses are recorded at 50 mV s^{-1} (positive side) and at 100 mV s^{-1} (negative side).

II). The cathodic and anodic currents are exactly equal and the quantity $i_p v^{-1/2}$ (i_p = peak current; v = scan rate) is found to be a constant. Coulometric data confirm the 1e stoichiometry (Table II). Formal potentials calculated as the average of peak potentials are in Table II. In the deprotonated species, the ruthenium(III)–ruthenium(II) couple (eq 5) is



again highly reversible but the formal potential ($\sim -0.2 \text{ V}$ vs. SCE) is shifted by $\sim 600 \text{ mV}$ from that of couple 4 toward a lower potential (Figure 2; Table III). Removal of a proton greatly facilitates metal oxidation. In fact, the observed E_{298}° values (Table III) are the lowest^{23,24} among complexes of

(20) We have observed that in a large group³ of $\text{Fe}(\text{RX})_3$, ν_{CO} lies in the region $1530\text{--}1600 \text{ cm}^{-1}$.

(21) Abu-Dari, K.; Raymond, K. N. *Inorg. Chem.* **1980**, *19*, 2034.

(22) Van Houten, J.; Watts, R. J. *Inorg. Chem.* **1978**, *17*, 3381.

(23) The lowest value (0.16 V) reported thus far pertains to²⁴ $\text{Ru}(\text{bpy})_2\text{L}^+$ where L^- is $\text{EtN}(\text{O})\text{N}=\text{N}(\text{C}_6\text{H}_4\text{-}p\text{-Me})^-$.

(24) Mukherjee, R. N.; Chakravorty, A. *J. Chem. Soc., Dalton Trans.* **1983**, 2197.

Table III. Electrochemical Results^{a,b} of Ru(bpy)₂(X)·H₂O in Acetonitrile at 298 K

X	metal oxidn ^{c,d} E°_{298}/V		bpy redn ^e $-E^{\circ}_{298}/V$ ($\Delta E_p/mV$)
	Ru(III)– Ru(II)	Ru(IV)– Ru(III)	
OMe	-0.30	0.80	1.65 (70), 1.95 (80)
H	-0.27	0.84	1.65 (70), 1.95 (70)
NO ₂ ^f	-0.21	0.89	1.64 (60), 1.93 (80)

^a Meaning of symbols are as in text. ^b Supporting electrolyte TEAP (0.1 M); solute concentration $\sim 10^{-3}$ M. ^c Platinum working electrode. ^d From cyclic voltammetry; scan rate 50 mV s⁻¹–1.0 V s⁻¹; $\Delta E_p = 60$ mV for both couples over the entire range of scan rates. ^e Glassy-carbon electrode, scan rate 100 mV s⁻¹. ^f Quasi-reversible 1e nitro reduction is observed at -1.20 V, $\Delta E_p = 80$ mV.

Ru(bpy)₂²⁺. Near 0.8 V, a second reversible ($\Delta E_p \sim 60$ mV; Figure 2; Table III) 1e couple is observed and this is assigned^{25,19} to the ruthenium(IV)–ruthenium(III) couple (6). The relative instability of the ruthenium(IV) complex is reflected in slow-scan CV²⁶ as well as in coulometric²⁷ data. The 1e stoichiometry of couples 5 and 6 is in full agreement with coulometric data.



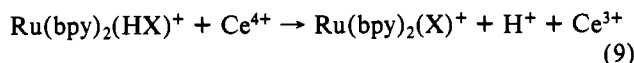
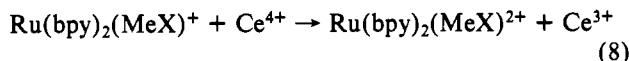
A search for the ruthenium(IV)–ruthenium(III) couple was made in the case of the Ru(bpy)₂(RX)⁺ species without success. All complexes of the types Ru(bpy)₂(RX)⁺ and Ru(bpy)₂(X) display an irreversible oxidation peak at ~ 1.70 V, the current height of which is much larger than that required for a 1e process (Figures 1 and 2). This response is probably due to ligand oxidation.²⁸

(b) **Hammett Correlation.** The formal potentials of couples 4, 5, and 6 obey the Hammett relationship (7) (Figure 3). In

$$\Delta E^{\circ}_{298} = \rho \sigma \quad (7)$$

eq 7 ΔE°_{298} is the shift in formal potential from the standard (X = H), ρ is the reaction constant, and σ is the substituent constant. The ρ value for the ruthenium complexes (~ 0.09 V) compares favorably with that of Fe(RX)₃ (~ 0.06 V).^{3,29} In hydroxamates, substituent X is seven bonds away from the metal. In the more common^{24,30,31} six-bond situation ρ values are usually larger (~ 0.2 V).

(c) **Chemical Oxidation: Isolation of Ruthenium(III) Species.** In neutral water–acetonitrile (80:20) medium, ceric ammonium sulfate brings about the reactions (8) and (9)



(25) In Ru(bpy)₂Cl₂ the corresponding couple¹⁹ is at 1.98 V; the ruthenium(III)–ruthenium(II) couple is at 0.33 V. The favorable effect of the hydroxamate chelates on the higher oxidation states of ruthenium is indeed striking.

(26) Thus, at $v = 20$ mV s⁻¹ the cathodic peak is smaller than the anodic peak; at $v = 100$ mV s⁻¹ the two peak heights are nearly equal (Figure 2).

(27) Coulometrically oxidized (at 1.2 V) solutions do not display any response in the region 0.0–1.0 V. The nature of the decomposition product has not been established.

(28) Similar oxidations are also displayed by MoO₂(RX)₂¹⁷ (~ 2.0 V), Fe(RX)₃³ (~ 2 V), and HRX (~ 1.8 V).

(29) In molybdenum hydroxamates,¹⁷ the ρ value is larger (~ 0.20 V); here, the substituent effect is transmitted better than in Fe(RX)₃ and ruthenium species. In this context it may be significant that 2a \leftrightarrow 2b resonance is also more pronounced in the molybdenum complexes (see text).

(30) Mukherjee, R. N.; Rajan, O. A.; Chakravorty, A. *Inorg. Chem.* **1982**, *21*, 785.

(31) Mukherjee, R. N.; Chakravorty, A. *J. Chem. Soc., Dalton Trans.* **1983**, 955.

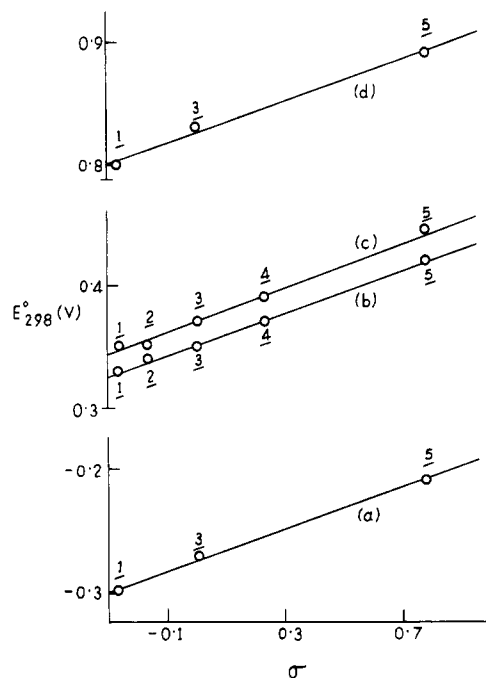
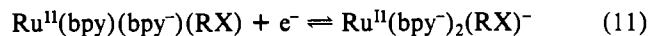
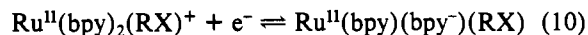


Figure 3. Least-squares fit of E°_{298} vs. σ : (a) ruthenium(III)–ruthenium(II) couple of Ru(bpy)₂(X)·H₂O ($\rho = 0.08$ V); (b) ruthenium(III)–ruthenium(II) couple of Ru(bpy)₂(MeX)·ClO₄·2H₂O ($\rho = 0.09$ V); (c) ruthenium(III)–ruthenium(II) couple of Ru(bpy)₂(HX)ClO₄·2H₂O ($\rho = 0.08$ V); (d) ruthenium(IV)–ruthenium(III) couple of Ru(bpy)₂(X)·H₂O ($\rho = 0.08$ V). The numbers in each figure refer to substituents X: OMe, 1; Me, 2; H, 3; Cl, 4; NO₂, 5.

quantitatively. The blue (reaction 8) and brownish yellow (reaction 9) complexes are isolated and characterized as perchlorates. Two representative examples are in Table I. Both are low spin as expected. The cyclic voltammetric behavior of Ru(bpy)₂(MeMe)²⁺ and Ru(bpy)₂(H)⁺ in acetonitrile is identical³² with that of Ru(bpy)₂(MeMe)⁺ (couple 4; R = X = Me) and Ru(bpy)₂(H) (couples 5 and 6; X = H), respectively.

(d) **Reductions of bpy.** 2,2'-Bipyridine has one electrochemically accessible LUMO. It thus gives rise to two successive reductions.³³ In the M(bpy)_n moiety, 2n reductions are possible in principle. The present complexes systematically display two of the four expected reductions above -1.5 V at a glassy-carbon electrode (Figures 1 and 2; Tables II and III). The processes are reversible or quasi-reversible ($\Delta E_p = 60$ –100 mV) in nature. The other two reductions are not observable due to solvent cutoff. The logical description of the observed processes is (similar equations apply to the complexes of deprotonated ligands) given by (10) and (11). The effect of



the X substituent on bpy reduction potentials is generally too small to be observed.³⁴ However, a drastic alteration on the hydroxamate ring such as deprotonation leads to a measurable change in bpy reduction potentials (Table II). Evidently the interaction between the RX and bpy rings is relatively small.

D. Electroprotic Equilibria. On the CV time scale eq 4 applies in acetonitrile for both R = Me and R = H. However on longer time scales spontaneous proton dissociation occurs

(32) Here the initial scan is cathodic whereas such a scan is anodic when the ruthenium(II) complexes are studied.

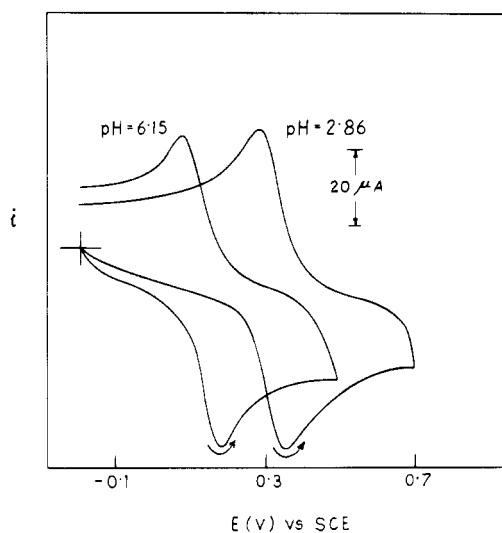
(33) Vlček, A. A. *Coord. Chem. Rev.* **1982**, *43*, 39.

(34) This is good indirect evidence that none of the two reductions occurs at the hydroxamate ring. In molybdenum(VI) hydroxamates¹⁷ such reductions are seen as irreversible waves below -2.0 V.

Table IV. Variable-pH Cyclic Voltammetric Results^{a,b} of Ru(bpy)₂(HX)ClO₄·2H₂O at a Glassy-Carbon Electrode in 60:40 Water-Dioxane Buffers

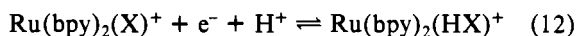
R	X	pH	\bar{E}_p/V ($\Delta E_p/mV$)	E°_{298}/V
H	H	6.15	0.13 (100)	0.49
		4.38	0.22 (110)	0.48
		2.86	0.31 (120)	0.48
H	OMe	7.72	0.01 (120)	0.47
		5.85	0.12 (120)	0.47
		4.35	0.21 (130)	0.47

^a Meaning of symbols are as in text. ^b Solute concentration $\sim 10^{-3}$ M; scan rate 100 mV s⁻¹.

**Figure 4.** Variable-pH cyclic voltammograms of Ru(bpy)₂(HH)ClO₄·2H₂O in 60:40 water-dioxane mixtures at a glassy-carbon electrode (scan rate 100 mV s⁻¹).

from the oxidized complex. Thus, a coulometrically oxidized (at 0.6 V) acetonitrile solution of Ru(bpy)₂(HX)⁺ contains Ru(bpy)₂(X)⁺ and not Ru(bpy)₂(HX)²⁺ as can be demonstrated from voltammetric (CV identical with that of Ru(bpy)₂(X)⁺) and spectroscopic (vide infra) examination of such solutions. Similarly, coulometric rereduction (at -0.5 V) of oxidized solutions leads to quantitative re-formation of Ru(bpy)₂(HX)⁺. In aqueous media proton transfer on metal oxidation becomes more facile as in eq 9.

The equilibrium (12) has been examined at a glassy-carbon electrode by CV in 60:40 water-dioxane buffers in the pH range³⁷ 7-2. In eq 12, electron and proton transfers are



coupled^{35,36} and we call this an *electroprotic equilibrium*. Results for two cases are in Figure 4 and Table IV. The quasi-reversible voltammograms shift to higher potentials with increasing acidity at the rate of approximately 60 mV/unit of pH. The formal potentials of couple 12 for two cases calculated at several pH values by adding the quantity 0.059pH to the average of peak potentials are in Table IV. Electroprotic equilibria are known⁸ to occur in some iron hydroxamates.

- (35) Mohanty, J. G.; Chakravorty, A. *Inorg. Chem.* **1976**, *15*, 2912. Singh, A. N.; Chakravorty, A. *Ibid.* **1980**, *19*, 969. Goswami, S.; Chakravorty, A. R.; Chakravorty, A. *J. Chem. Soc., Chem. Commun.* **1982**, 1288.
- (36) Dryhurst, G. "Electrochemistry of Biological Molecules"; Academic Press: New York, 1977. Beinert, H. *Coord. Chem. Rev.* **1980**, *33*, 55. Williams, R. J. P. *Chem. Soc. Rev.* **1980**, *9*, 281. Mitchell, P. *Chem. Ber.* **1981**, *17*, 14.
- (37) Since Ru(bpy)₂(HH)⁺ itself undergoes proton dissociation (pK = 9.90) in alkaline medium, the pH was kept low enough to hold the whole of the ruthenium(II) complex in the protonated form.

Table V. Electronic Spectral Data^a

R	X	λ/nm ($\epsilon/M^{-1} \text{ cm}^{-1}$)
Ru(bpy) ₂ (RX)ClO ₄ ·2H ₂ O		
Me	OMe	590 ^d (2900), 535 (4200), 470 ^d (3900), 345 (5900), 295 (44 700), 245 (30 400), 215 (11 000)
Me	H	590 ^d (3500), 535 (5000), 470 ^d (4200), 342 (6900), 295 (31 500), 240 (22 000), 215 (12 000)
Me	NO ₂	590 ^d (3600), 525 (6300), 470 ^d (5800), 325 (6200), 295 (48 000), 245 (32 000), 215 (11 500)
H	H	590 ^d (3600), 535 (5500), 470 ^d (4000), 345 (6500), 295 (40 000), 245 (30 000)
H	NO ₂	585 ^d (3000), 530 (6200), 470 ^d (5600), 340 (7000), 295 (50 000), 245 (33 000)
Ru(bpy) ₂ (X)·H ₂ O		
H	H	720 ^d (2500), 610 (6000), 470 ^d (5600), 380 (9700), 290 (37 500), 250 (26 000)
Ru(bpy) ₂ (RX)(ClO ₄) ₂ ·2H ₂ O ^b		
Me	OMe	620 (4500), 460 ^d (3000), 360 ^d (5000), 290 (25 000), 245 (28 000)
Me	Me ^c	620 (4000), 470 ^d (4000), 370 (5500), 285 (33 900), 245 (23 000)
Me	H	620 (4200), 470 (3000), 355 (7000), 290 (33 000), 245 (22 000)
Ru(bpy) ₂ (X)ClO ₄ ·2H ₂ O ^b		
Me	Me	730 (4000), 460 (3000), 345 ^d (6000), 295 (32 000), 245 (29 500)
H ^c	H	735 (3500), 460 (4000), 340 (6500), 295 (31 500), 245 (30 000)
NO ₂	NO ₂	725 (5000), 450 (6000), 330 ^d (8000), 295 (35 000), 245 (25 000)

^a Solvent is acetonitrile. ^b Unless otherwise stated, electronic spectral data were collected by using coulometrically generated species. ^c Measurements are made after dissolving the pure solid compound in acetonitrile. ^d Shoulder.

We note that eq 12 can be written as the sum of eq 3 and 5 and it is then possible to write³⁸ eq 13. Here, $E^{\circ}_{298}(5)$ is

$$E^{\circ}_{298}(12) = E^{\circ}_{298}(5) + 0.059pK \quad (13)$$

the E°_{298} of equilibrium 5. For X = H, we have pK = 9.90, $E^{\circ}_{298}(12) = 0.48$ V, and hence $E^{\circ}_{298}(5)$ is estimated with the help of eq 13 to be -0.1 V. This value refers to water-dioxane and is higher than the experimental value in acetonitrile.³⁹

E. MLCT Spectra: Correlation with Redox Potentials. The Ru(bpy)₂(RX)⁺ complexes show an allowed transition at ~ 530 nm with a shoulder at ~ 590 nm (Figure 5; Table V). A d(Ru) \rightarrow π^* (bpy) assignment for the band system is logical.⁴⁰ On going from Ru(bpy)₂(HX)⁺ to Ru(bpy)₂(X), the band system undergoes a pronounced red shift. This is expected on several counts. For example, the effective positive charge on the metal atom would decrease on proton loss, resulting in destabilization of metal orbitals. The bpy orbitals will no doubt be affected also but to a much lesser extent. In this context we recall the observed large decrease in metal redox potential and the relatively smaller change of bpy redox potentials on deprotonation.

We now briefly examine the interrelationship of the above two redox potentials with the energy of MLCT bands in the hydroxamates as well as in other selected complexes of Ru(bpy)₂²⁺. For this purpose, the quantity ΔE° is defined as in eq 14 where $E^{\circ}(\text{Ru})$ is the ruthenium(III)-ruthenium(II)

$$\Delta E^{\circ} = E^{\circ}(\text{Ru}) - E^{\circ}(\text{bpy}) \quad (14)$$

(38) Mohanty, J. G.; Chakravorty, A. *Inorg. Chem.* **1977**, *16*, 1561.

(39) A similar situation obtains in molybdenum hydroxamates,¹⁷ which however do not display electroprotic equilibria. Here, proton removal blocks the electron-transfer path.

(40) Ceulemans, A.; Vanquickenborne, L. G. *J. Am. Chem. Soc.* **1981**, *103*, 2238. Felix, F.; Ferguson, J.; Güdel, H. U.; Ludi, A. *Ibid.* **1980**, *102*, 4096. Decurtins, S.; Felix, F.; Ferguson, J.; Güdel, H. U.; Ludi, A. *Ibid.* **1980**, *102*, 4102.

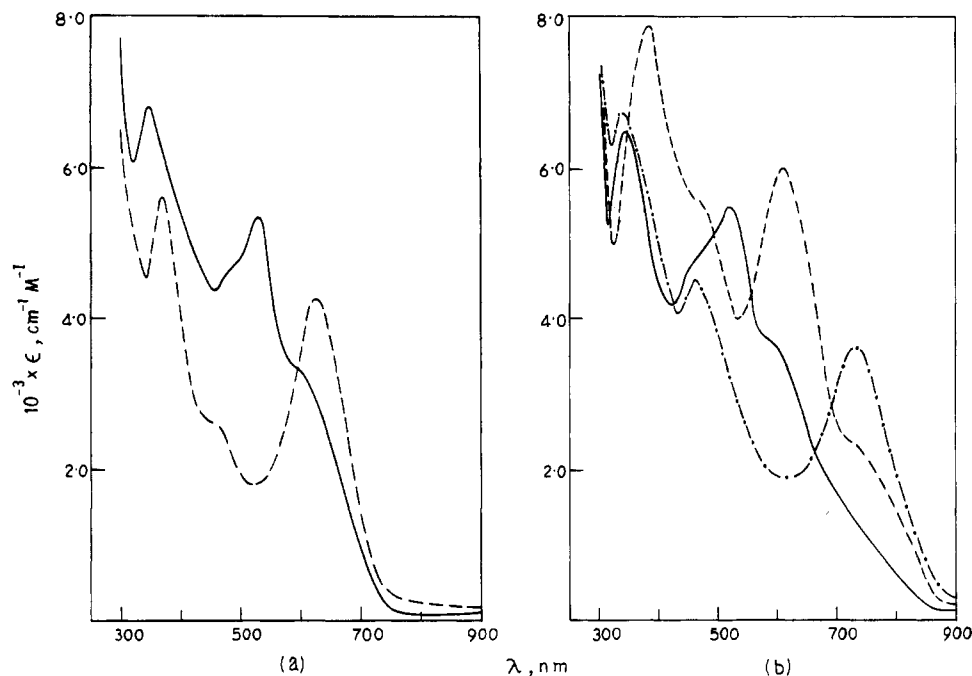


Figure 5. Electronic spectra in acetonitrile: (a) (—) $\text{Ru}(\text{bpy})_2(\text{MeH})\text{ClO}_4 \cdot 2\text{H}_2\text{O}$, (---) $\text{Ru}(\text{bpy})_2(\text{MeH})(\text{ClO}_4)_2 \cdot 2\text{H}_2\text{O}$; (b) (—) $\text{Ru}(\text{bpy})_2(\text{HH})\text{ClO}_4 \cdot 2\text{H}_2\text{O}$, (---) $\text{Ru}(\text{bpy})_2(\text{H}) \cdot \text{H}_2\text{O}$, (-.-) $\text{Ru}(\text{bpy})_2(\text{H})\text{ClO}_4 \cdot 2\text{H}_2\text{O}$.

formal potential and $E^\circ(\text{bpy})$ refers to the bpy reduction occurring at highest potential (e.g., eq 10). The energy (ν_{min} in cm^{-1}) of the MLCT transition occurring at lowest energy is found to correlate linearly with ΔE° of a number of species^{24,41-44} of the type $\text{Ru}(\text{bpy})_2(\text{bidentate})^{x+}$ (Table VI). The ranges of ΔE° (2.69–1.48 V) and ν_{min} (23 000–14 000 cm^{-1}) covered are quite large. From eq 15 it is possible to predict

$$\nu_{\text{min}} = 8065\Delta E^\circ + 1200 \quad (15)$$

ν_{min} to within $\pm 1000 \text{ cm}^{-1}$ of the experimental value in most cases. In eq 15, the factor 8065 is used to convert V to cm^{-1} and 1200 is taken as an empirical term for the present.

The applicability of eq 15 extends also to species where $\text{Ru}(\text{bpy})_2^{2+}$ is coordinated to monodentate ligands⁴⁵⁻⁴⁷ (Table VI). This is not to claim⁴⁸ that all published data obey eq 15. At this time eq 15 is advanced merely as a useful empirical equation. We however note that equations similar to (15) can be devised for successful application to complexes of 2-(arylazo)pyridine,⁴⁹ 2,2'-bipyrazine, 2,2',2''-terpyridine, and a host of other unsaturated ligands. In fact a single equation of type (16) where α and β are constants can be constructed to en-

$$\nu_{\text{min}} = \alpha E^\circ + \beta \quad (16)$$

compass a surprisingly large volume of available spectral and redox data. The thermodynamic basis of equations like (15)

Table VI. Spectroelectrochemical Data^{a,b}

complex ^c	$\Delta E^\circ/\text{V}$	$\nu_{\text{min}}/\text{cm}^{-1}$		ref
		calcd ^d	obsd	
$\text{Ru}(\text{bpy})_2(\text{H})$	1.48	13 140	13 890	this work
$\text{Ru}(\text{bpy})_2(\text{T})^+$	1.85	16 120	16 230	24
$\text{Ru}(\text{bpy})_2(\text{HH})^+$	1.94	16 850	16 950	this work
$\text{Ru}(\text{bpy})_2(\text{bq})^{2+}$	2.24	19 270	19 010	41
$\text{Ru}(\text{bpy})_2(\text{L})^+$	2.34	20 070	20 620	42
$\text{Ru}(\text{bpy})_2(\text{phen})^{2+}$	2.62	22 330	22 370	41
$\text{Ru}(\text{bpy})_3^{2+}$	2.69	22 900	22 270	43
$\text{Ru}(\text{bpy})_2(\text{acac})^+$	2.11	17 900	18 600	44 ^e
$\text{Ru}(\text{bpy})_2\text{Cl}_2$	1.99	17 250	18 080	45
$\text{Ru}(\text{bpy})_2(\text{CN})_2^{2+}$	2.39	20 480	19 490 ^f	46
$\text{Ru}(\text{bpy})_2(\text{MePh}_2\text{P})^{2+}$	2.83	24 030	23 420	47
$\text{Ru}(\text{bpy})_2^-$	3.03	25 640	26 810	47
$(\text{cis-Ph}_2\text{PCH=CHPh}_2)^{2+}$				

^a Meaning of symbols are as in text. ^b Unless otherwise stated, the voltammetric and spectral data are in acetonitrile. ^c Abbreviations: T, triazine 1-oxide; bq, 2,2'-biquinoline; L, isonitroso-ketone, $\text{R}'\text{C}(\text{=O})\text{C}(\text{=NOH})\text{R}$ (R, R' = alkyl or aryl group); py, pyridine; phen, 1,10-phenanthroline; acac, acetylacetonate.

^d Calculated by using eq 15 (see text). ^e In ref 44 the electronic spectrum of $\text{Ru}(\text{bpy})_2(\text{acac})^+$ is reported in dichloromethane. The tabulated ΔE° and ν_{min} values were measured by us in acetonitrile. ^f In dimethylformamide.

and (16) and the range of their applicability will be critically examined elsewhere.⁵⁰

F. Concluding Remarks. The binding of bidentate hydroxamic acids to bis(bipyridine) chelates of ruthenium(II), ruthenium(III), and ruthenium(IV) has been demonstrated through isolation and/or voltammetric studies. The complexes display an impressive array of equilibria and correlations involving proton transfer, electron transfer, and spectroscopic charge transfer.

The stability of high-spin iron(III) hydroxamates is far in excess of that of the corresponding iron(II) species.⁵¹ Though stability constant data for the ruthenium complexes are not

- (41) Belsler, P.; Zelewsky, A. *Helv. Chim. Acta* **1980**, *63*, 1675.
 (42) Chakravarty, A. R.; Chakravorty, A. *J. Chem. Soc., Dalton Trans.* **1982**, 1765.
 (43) Weiner, M. A.; Basu, A. *Inorg. Chem.* **1980**, *19*, 2797.
 (44) Bryant, G. M.; Fergusson, J. E.; Powell, H. K. *J. Aust. J. Chem.* **1971**, *24*, 257.
 (45) Sullivan, B. P.; Salmon, D. J.; Meyer, T. J.; Peedin, J. *Inorg. Chem.* **1979**, *18*, 3369.
 (46) Kalyansundaram, K. *Coord. Chem. Rev.* **1982**, *21*, 3849.
 (47) Sullivan, B. P.; Salmon, D. J.; Meyer, T. J. *Inorg. Chem.* **1978**, *17*, 3334.
 (48) (a) In fact the question of such a claim does not arise since it would be hard to find a physical basis for it. As stated in the text in connection with eq 16 this aspect of the problem will be considered elsewhere.⁵⁰ (b) A notable exception to eq 15 is provided by species of the type $\text{Ru}(\text{bpy})_2\text{BX}^+$ where B is a tertiary phosphine or arsine and X is a halide. Reported data⁴⁷ lead to calculated ν_{min} values that are too low (by 2000–3000 cm^{-1}).
 (49) Goswami, S.; Mukherjee, R. N.; Chakravorty, A. *Inorg. Chem.* **1983**, *22*, 2823.

- (50) Mukherjee, R. N.; Goswami, S.; Ghosh, P.; Chakravorty, A., unpublished results.
 (51) Martell, A. E.; Smith, R. M. "Critical Stability Constants"; Plenum Press: New York, 1977; Vol. 3. Carrano, C. J.; Cooper, S. R.; Raymond, K. N. *J. Am. Chem. Soc.* **1979**, *101*, 599.

available, it is clear that hydroxamates in general and hydroximates in particular lead to low ruthenium(III)–ruthenium(II) redox potentials. In the case of hydroximates this potential as well as the ruthenium(IV)–ruthenium(III) potential falls below all reported values for the complexes of the Ru(bpy)₂ moiety. The stabilizing influence of the present ligands on the higher oxidation states of ruthenium is indeed impressive. In this respect the behavior of the 3+ states of iron and ruthenium—even though they have different spin multiplicities—is parallel, suggesting that the electrostatic component in metal–hydroxamate interaction may be considerable. The synthesis of tris(hydroxamates) and tris(hydroximates) of ruthenium^{13,18} is of obvious interest. The redox potentials of such species can be expected to be very low, and the isolation of a ruthenium(IV) complex may then become possible. We are investigating this problem as well as the chemistry of the hydroxamates of osmium. Finally, we comment on the electronic spectra of ruthenium(III) chelates (Table V). Spectra were collected either by dissolving pure complexes or by coulometrically generating the chelates in situ. A dominating feature is the allowed band near 620 nm in Ru(bpy)₂(MeX)²⁺ or near 730 nm in Ru(bpy)₂(X)⁺ (Figure 5). This band is tentatively assigned to hydroxamate (hydroximate) → Ru transition. Transitions of the type bpy → Ru are known^{24,46,52} to be relatively weak. The availability of tris(hydroxamates) will help in confirming the proposed assignment.

Experimental Section

Materials. The purification of solvents and preparation of supporting electrolytes for electrochemical works were done as before.⁵¹ Water of high purity was obtained by distillation of deionized water from KMnO₄. Sodium chloride for pH-metric works was recrystallized from water. Dinitrogen was purified by bubbling it through an alkaline dithionite reducing solution. Cerium(IV) solutions were prepared from reagent grade ceric ammonium sulfate. All other chemicals used for the preparative works were of reagent grade and were used without further purification.

Measurements. Electronic spectra were obtained by using a Cary 17D or a Pye Unicam SP8-150 spectrophotometer. Infrared spectra (KBr disk, 4000–400 cm⁻¹) were collected with a Beckman IR-20A spectrophotometer. Solution electrical conductivity was measured by using a Philips PR 9500 bridge with a solute concentration of ~10⁻³ M. Magnetic moments were measured with the help of a PAR 155 vibrating-sample magnetometer. Cyclic voltammetry was performed under a dinitrogen atmosphere with the help of a PAR Model 370-4 electrochemistry system having among other things a 174A polarographic analyzer, a 175 universal programmer, and a RE 0074 X-Y recorder. In the three-electrode configuration either a Beckman Model 39273 platinum electrode or a PAR Model G0021 glassy-carbon electrode was the working electrode. For controlled-potential coulometry a Model 173 potentiostat, 179 digital coulometer, and 377A cell system having a platinum-wire-gauge electrode was used. All measurements were made at 298 K. The potentials are referenced to the saturated calomel electrode and are uncorrected for junction contribution.

The following σ values⁵³ for para substituents were used: OMe, -0.27; Me, -0.17; H, 0.00; Cl, +0.23; NO₂, +0.78.

For the pH-dependent electrochemical measurements, acetate and phosphate buffers were used. The voltammograms were taken in 60:40 buffer–dioxane mixtures. The pH of each such mixture was recorded with the help of a Type 335 Systronics pH meter. The electrolytes in their buffers also acted as supporting electrolytes.

Determination of pK Values. The pH-metric titrations were done under a dinitrogen atmosphere on 10 mL of 10⁻² M Ru(bpy)₂-

(XHL)ClO₄·2H₂O in 60:40 water–dioxane (1.0 M in NaCl) at 298 K. Carbonate-free sodium hydroxide solution (0.0369 N) was added from a buret that could be read accurately to 0.01 mL. For equilibrium 3, (17) holds, where a is the total concentration of the complexes,

$$pK = \text{pH} - \log \frac{[\text{Na}^+]}{a - [\text{Na}^+]} \quad (17)$$

[Na⁺] is the concentration of Na⁺ coming from added NaOH, and K is the equilibrium constant of reaction 3. The pK values were computed from (17) at various levels of neutralization.

Synthesis of Compounds. Bis(2,2'-bipyridine)(carbonato)ruthenium(II) Dihydrate, Ru(bpy)₂CO₃·2H₂O. It was prepared by following a published procedure.¹⁹ Hydroxamic acids were prepared by acylation of hydroxylamines with acid chlorides. *Caution!* Perchlorate salts reported below may explode.

Bis(2,2'-bipyridine)(benzohydroxamato)ruthenium(II) Perchlorate Dihydrate, Ru(bpy)₂(HH)ClO₄·2H₂O. Violet Ru(bpy)₂CO₃·2H₂O (100 mg, 0.20 mmol) was dissolved in 10 mL of a 1:1 ethanol–water mixture. To it was added 60 mg (0.44 mmol) of benzohydroxamic acid. The mixture was magnetically stirred at 298 K under a dinitrogen atmosphere for 3 h. To the filtrate was added saturated ice-cold NaClO₄ (25 mL, deaerated) solution. Immediately, a pink solid separated out, which was collected by filtration and washed thoroughly with ice-cold water. The product was dried in vacuo over P₄O₁₀ and then recrystallized from dichloromethane–hexane. The yield of pure product was 40%.

The various other Ru(bpy)₂(HX)(ClO₄)·2H₂O species were prepared similarly.

Bis(2,2'-bipyridine)(N-methylbenzohydroxamato)ruthenium(II) Perchlorate Dihydrate, Ru(bpy)₂(MeH)ClO₄·2H₂O. The complex Ru(bpy)₂CO₃·2H₂O (100 mg, 0.20 mmol) was dissolved in 10 mL of water with constant bubbling of dinitrogen. To it was added 2 mL of 2 N H₂SO₄. After 5 min 2 N NaOH was allowed to run into the solution until the pH of the solution became ~10. Then, N-methylbenzohydroxamic acid (35 mg, 0.23 mmol) was added, and the mixture was magnetically stirred at 298 K for 1 h. The subsequent isolation and recrystallization procedures were essentially the same as described for the previous complex. The yield was 75%.

The complexes with other substituents (X) were prepared similarly.

Bis(2,2'-bipyridine)(benzohydroximato)ruthenium(II) Monohydrate, Ru(bpy)₂(H)·H₂O. To a solution of 80 mg of Ru(bpy)₂(HH)ClO₄·2H₂O in 20 mL of water under dinitrogen was added 5 mL of 4 N NaOH. The reaction mixture was stirred for 2 h. The bottle green colored complex was extracted repeatedly with chloroform (6 × 25 mL). The volume of the extract was then brought to 10 mL under reduced pressure. The concentrate was then titrated with 40 mL of hexane. The needle-shaped complex that separated was filtered off and dried over P₄O₁₀. The yield was 60%.

The complexes with other substituents (X) can be synthesized similarly.

Bis(2,2'-bipyridine)(N-methyl-p-tolylhydroxamato)ruthenium(III) Diperchlorate Dihydrate, Ru(bpy)₂(MeMe)(ClO₄)₂·2H₂O. To a solution of 80 mg (0.115 mmol) of Ru(bpy)₂(MeMe)ClO₄·2H₂O in 15 mL of water–acetonitrile (80:20) was added dropwise 10 mL of aqueous solution of ceric ammonium sulfate (40 mg, 0.086 mmol) under magnetic stirring. Stirring was continued for 1 h. Excess NaClO₄ (solid) was then added. A light blue solid separated out. The product was washed with ice-cold water and collected by filtration. The yield of the dried product was 70%.

Bis(2,2'-bipyridine)(benzohydroximato)ruthenium(III) Perchlorate Dihydrate, Ru(bpy)₂(H)ClO₄·2H₂O. This brownish yellow complex was isolated by following the same procedure as above with Ru(bpy)₂(HH)ClO₄·2H₂O as starting material. The yield was 40%.

In the infrared spectrum, stretching (~3500 cm⁻¹ (br, s)) and bending (~1640 cm⁻¹ (sp, m)) modes of water and the ionic perchlorate bands (~1150 cm⁻¹ (br, s), 620 cm⁻¹ (sp, s)) are observed in addition to numerous bands due to the organic ligands.

Acknowledgment. Financial support received from the Department of Science and Technology, New Delhi, is gratefully acknowledged.

(52) Bryant, G. M.; Fergusson, J. E. *Aust. J. Chem.* **1971**, *24*, 275.

(53) Hammett, L. P. "Physical Organic Chemistry", 2nd ed.; McGraw Hill: New York, 1970.